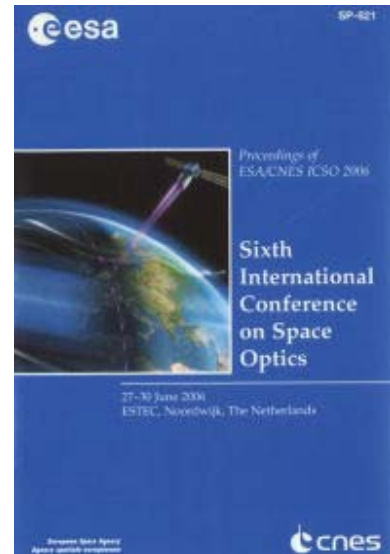


# International Conference on Space Optics—ICSO 2006

Noordwijk, Netherlands

27–30 June 2006

*Edited by Errico Armandillo, Josiane Costeraste, and Nikos Karafolas*



## *X-ray pore optic developments*

*Kotska Wallace, Marcos Bavdaz, Maximilien Collon, Marco Beijersbergen, et al.*



International Conference on Space Optics — ICSO 2006, edited by Errico Armandillo, Josiane Costeraste, Nikos Karafolas, Proc. of SPIE Vol. 10567, 105670U · © 2006 ESA and CNES  
CCC code: 0277-786X/17/\$18 · doi: 10.1117/12.2308040

Proc. of SPIE Vol. 10567 105670U-1

## X-RAY PORE OPTIC DEVELOPMENTS

Kotska Wallace<sup>(1)</sup>, Marcos Bavdaz<sup>(2)</sup>, Maximilien Collon<sup>(3)</sup>, Marco Beijersbergen<sup>(3)</sup>, Stefan Kraft<sup>(3)</sup>,  
Ray Fairbend<sup>(4)</sup>, Julien Séguy<sup>(4)</sup>, Pascal Blanquer<sup>(4)</sup>, Roland Graue<sup>(5)</sup>, Dirk Kampf<sup>(5)</sup>

<sup>(1)</sup> ESA, ESTEC, Mechatronics and Optics, Keplerlaan 1, PO Box 299, 2200 AG Noordwijk ZH, The Netherlands,  
Email: kotska.wallace@esa.int

<sup>(2)</sup> ESA, ESTEC, Science Payload and Advanced Concepts Office, Keplerlaan 1, PO Box 299, 2200 AG Noordwijk ZH,  
The Netherlands, Email: marcos.bavdaz@esa.int

<sup>(3)</sup> cosine Research BV, Niels Bohrweg 11, 2333 CA Leiden, The Netherlands, Email: m.collon@cosine.nl,  
m.beijersbergen@cosine.nl

<sup>(4)</sup> Photonis, Av. Roger Roncier, B.P. 250, 19106 Brive La Gaillarde Cedex, France, Email: r.fairbend@photonis.com,  
j.seguy@photonis.com

<sup>(5)</sup> Kayser-Threde GmbH, Optical Systems, Wolfratshauer Str. 48, D-81379, München, Germany;  
Email: roland.graue@kayser-threde.com, dirk.kampf@kayser-threde.com

### ABSTRACT

In support of future x-ray telescopes ESA is developing new optics for the x-ray regime. To date, mass and volume have made x-ray imaging technology prohibitive to planetary remote sensing imaging missions. And although highly successful, the mirror technology used on ESA's XMM-Newton is not sufficient for future, large, x-ray observatories, since physical limits on the mirror packing density mean that aperture size becomes prohibitive. To reduce telescope mass and volume the packing density of mirror shells must be reduced, whilst maintaining alignment and rigidity. Structures can also benefit from a modular optic arrangement. Pore optics are shown to meet these requirements. This paper will discuss two pore optic technologies under development, with examples of results from measurement campaigns on samples.

One activity has centred on the use of coated, silicon wafers, patterned with ribs, that are integrated onto a mandrel whose form has been polished to the required shape. The wafers follow the shape precisely, forming pore sizes in the sub-mm region. Individual stacks of mirrors can be manufactured without risk to, or dependency on, each other and aligned in a structure from which they can also be removed without hazard. A breadboard is currently being built to demonstrate this technology.

A second activity centres on glass pore optics. However an adaptation of micro channel plate technology to form square pores has resulted in a monolithic material that can be slumped into an optic form. Alignment and coating of two such plates produces an x-ray focusing optic. A breadboard 20cm aperture optic is currently being built.

### 1. BACKGROUND

In the energy regime of interest, 0.1 to 10 keV, only grazing incidence reflections can be exploited to focus an x-ray image. In the design of a Wolter I optic the two grazing incidence reflections (around 1°), from a parabolic then a hyperbolic surface, produce a real image of the x-ray source. In order to increase the effective area of an x-ray optic, the aperture must be packed densely with concentric shells of grazing incidence mirrors, traditionally formed from glass or nickel plates, stacked in a nested structure. To increase effective area the mirror shells must be as thin as possible, which consequentially makes them fragile, prone to distortion, difficult to align and mount. Shell mounts also constrain the inter-plate separation that can be achieved.

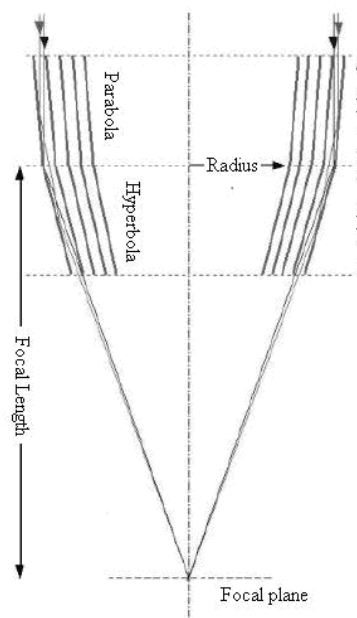


Fig. 1-1: Conical approximation of the parabolic and hyperbolic sections of a Wolter I optic to focus x-rays.

It is easier to manufacture a Wolter I optic using conical approximations to the surface shapes. The negative effect on imaging resolution can be minimised if the reflecting surfaces are kept small compared to the focal length. The azimuthal divergence of each of the mirror pore walls from spherical is also acceptable as long as the width of each pore is smaller than the required focal spot size. Therefore, although a pore optic provides a concentric series of flat reflecting surfaces, it allows rays to be focused when the system is manufactured with small pores. Small pore size also results in short optics. The pores form a series of concentric rings where the reflecting surfaces' inclinations change with respect to radial distance from the aperture centre, resulting in an x-ray focusing optic (Fig. 1-1).

Eqn. 1 gives the effective collecting area of the x-ray optic aperture for photons of energy, E, and an angle of incidence,  $\alpha$ .

$$A(E) \approx \sum 2\pi r \cdot L \cdot \tan(\alpha) \cdot R^2(\alpha, E) \quad (1)$$

where the summation is over all the stacked shells, L is the length of the mirror plates and r is the radial distance from the optic centre. Although the length of each reflecting surface should be dictated by its radial position, in reality the optic is manufactured from a number of plates of uniform thickness. Each section of pore optic has a thickness calculated to maximise reflections, whilst minimising vignetting, for the preferred pore lengths over the radial distances contained within it.  $R(\alpha, E)$  is the reflection coefficient of the surface material and results in a desire to coat the reflecting surfaces of the pores in a material that maximises reflection within the energy range of interest. Surfaces can be coated with a material such as nickel or iridium with a uniform thickness between 20-200nm and a surface roughness less than 2nm rms.

Pore optics allow significant light-weighting of an x-ray optic whilst retaining density of reflecting surfaces and therefore collecting area. In addition a monolithic structure is easier to mount than more traditional x-ray reflecting shells and its robustness makes it easier to protect regarding thermal variation, vibration and other mechanical stresses. The extent of the benefit means that instruments that were previously inconceivable within the limited accommodation provided by, for instance, a planetary surveyor spacecraft, can now be planned for the x-ray regime. The Mercury X-ray Spectrometer (MIXS) is one such instrument, planned for flight on ESA's BepiColombo spacecraft [1,2]. X-rays emitted from the Hermean surface, due to x-ray fluorescence from its interaction with solar x-rays, will be collected by a glass micro-pore optic. Intensity and spectral distribution of the incident solar x-rays vary

with the strength of solar output, increasing with solar flares. Using multi-spectral x-ray imaging should allow scientists to determine abundances of Na, Mg, Al, Si, Ca, K and Fe. This places a requirement on the instrument to cover the energy range 0.5-7.5 keV with an energy resolution of the detector of less than 200 eV. In order to meet tight mass and volume constraints a robust, compact optic element for the instrument is required and glass micro-pore optics are being developed to meet these requirements.

Other large, observatory missions, such as XEUS [3,4], are planned to investigate the nature of gravity, space and time with observations of matter under extreme conditions, for instance in collapsed galaxy clusters and massive black-holes. XEUS requires a large effective aperture of the order 5m<sup>2</sup> at 1 keV and an angular resolution below 5'' (with a goal of 2''). Glass micro-pore optic technology cannot, at this time, offer such resolution, although its use can be considered to construct a lightweight, rugged collimator in front of the x-ray optic mirrors to prevent straylight from entering the system. The above mentioned novel technique to form silicon milli-pore optics is being developed to meet these demanding requirements on resolution and effective area.

### 1.1 Technology development

ESA has supported pore optic developments in an effort to develop robust x-ray optics that are easy to mount, yet offer a low mass per collecting area. The development of x-ray micro-pore optics from glass MCPs is based on manufacturing processes and techniques used in the production of material for night vision applications [5]. The development has addressed the change from round to square pores, radial stacking and fusing to form segments of an optic, etching of higher aspect ratio fibres (length to diameter) and slumping of sectors to the required curve in order to approximate half of a Wolter I tandem. The development of x-ray milli-pore optics takes advantage of the newly developed and commercially available, highly polished 300mm wafers, required for the next generation of high performance integrated circuits. The production methods are designed for the large volumes required by the semiconductor industry and, therefore, the huge development costs for science and research are efficiently reduced for use in space project. The starting material provides a superb surface finish and surface topography. In addition, the properties of silicon itself are very favorable for the construction of x-ray optics: good thermal conductivity, excellent uniformity, good mechanical characteristics and ease of processing methods.

## 2. GLASS MICRO-PORE OPTICS

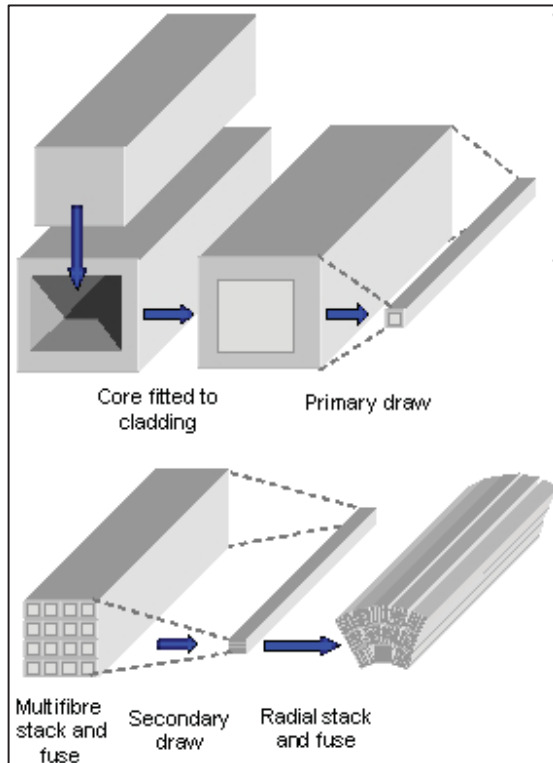


Fig. 2-1: Manufacturing steps to produce MCP material

Glass Micro Channel Pore (MCP) material is formed in a process which uses glass fibres Fig. 2-1. In the case for forming x-ray optics a method has been developed to draw square fibres from finely polished blocks of core glass which are encased in a precision fitted cladding glass. Development of the draw tower and dedicated metrology and inspection during automated manufacturing processes is described in [6]. The square fibres resulting from this primary draw are then restacked into a former and fused under heat and pressure. The resulting block of material undergoes a secondary draw to form Multi Fibre (MF) which consists of many microfibres. MFs are stacked in a radial configuration in a special former and fused (Fig. 2-2). Plates are sliced from the block and etched in acid to remove the core glass from the fibres. The remaining fibre cladding forms the walls of the square pores. The etch process has been optimised to reduce the roughness of the pore walls and increase reflectivity. The glass, micro pore plate can now be slumped on a former to obtain the desired curve that approximates a hyperbola or parabola. Two such plates can be aligned to form a Wolter I optic.

Pore sizes are typically 20 - 50 $\mu$ m with pore walls less than 10 $\mu$ m thick. However the monolithic structure is very rigid. Radial walls support the surfaces from

which the x-rays will be reflected to form a focus (top walls of the square channels in a radial stack) and ensure that these are stiff enough that the mirrors maintain the required shape. The mounting procedure requires only that the tandem is aligned together and optic segments aligned to form the aperture; i.e. no need to mount each shell.

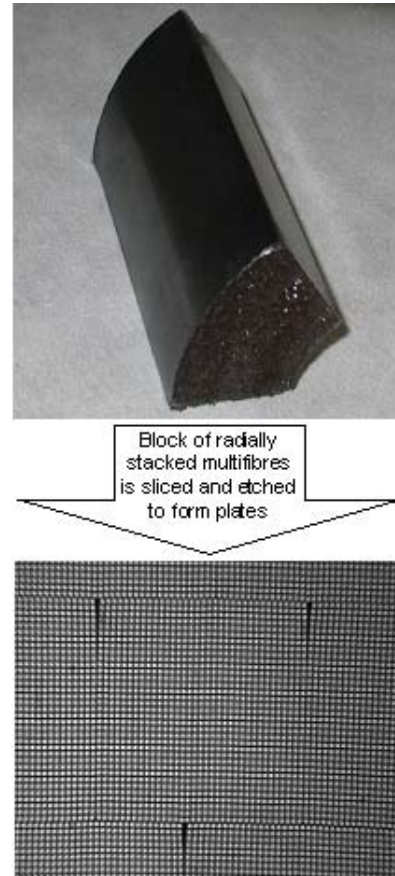


Fig. 2-2: Fused block of radially stacked micro-pore material above. Microscope image of sliced & etched plate below, one MF visible with surrounding MFs

Technology development activities have increased:

- accuracy of fibre alignment within MFs
  - accuracy of MF alignment within the radial stack
- Another problem which has been addressed is channel shear during slumping, which can occur instead of the formation of the desired confocal arrangement of micro channels. A series of specific thermal slumping tools has been developed for curving a series of off-axis radial segments (Fig. 2-3). The plates are slumped to form a doublet composed of one plate with radius 1.333m and one with radius 4.000m. The slumping tool is composed of two parts, a lower concave tool and a convex upper tool. Four pairs of tools have been made, having radii of 1.333  $\pm$  0.005m and 4.000  $\pm$  0.005m, for channel plate thicknesses of 2.5 and 5mm.

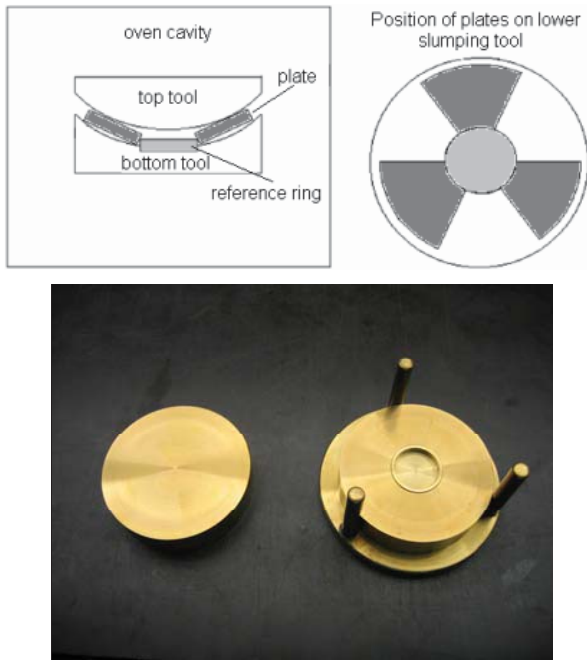


Fig. 2-3: Schematic of radial plate positions in the slumping mould and photo of the mould used.

An oven with an automatic, computer controlled, slumping procedure allows precise control of the temperature profile, the slumping force and the slumping rate, which is necessary to produce the correct radial disposition of the individual channel orientations within the micro-pore optic plates. Using a co-ordinate measuring machine, measurements on slumped test samples of round pore material have shown that the radius of curvature achieved is within  $180\mu\text{m}$  of the expected curvature for 2.5mm thick plates and  $50\mu\text{m}$  of the expected curvature for 5mm thick plates.

X-ray measurements on single, unslumped test plates have shown co-alignment of fibres to produce overlaid x-ray spots with Half Energy Width (HEW) around  $50''$  and it is expected that the requirement of a 200mm aperture optic, with better than  $1'$  resolution over a  $1^\circ$  field of view, can be met<sup>(11)</sup>. Tests will now be conducted on slumped and aligned plates that form tandem pairs. Coating has also been demonstrated and has achieved penetration depths with aspect ratios of 1000 in  $20\mu\text{m}$  pore material using an electroless deposition method.

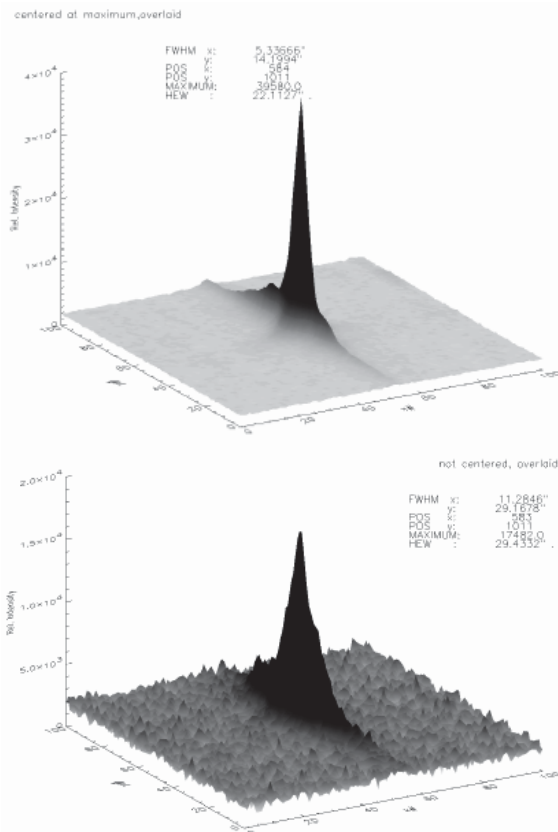


Fig. 2-4: Results of tests with a 3keV,  $100\mu\text{m}$  pencil beam  
Overlaid spots reflected through  $46\mu\text{m}$  square pore multifibre;  $1\text{px} = 1.77''$ . Spots centred on their maxima (top, HEW  $22''$ ) and raw images overlaid (bottom, HEW  $29''$ )

### 3. SILICON MILLI-PORE OPTICS

Silicon milli-pore optics are formed by stacking commercially available, polished silicon wafers<sup>8</sup>, which are used by the semiconductor industry and therefore manufactured in large-scale production. High grade wafers are available with extremely low surface roughness, less than 1 nm, achieved via surface chemo-mechanical polishing or deposition of epitaxial layers. The wafers are first diced into smaller squares and those are then cut with grooves to form a rib structure. They are then cylindrically deformed and assembled on a mandrel to form a very stiff, porous structure consisting of many of x-ray mirrors. When two plates are integrated they form Van der Waals bonds to each other and the stack thereby can retain its shape when free-standing. The mirror performance of stacks of up to 20 plates with an outer radius of curvature of 2m has been characterised<sup>9</sup> at an x-ray facility and has reached, on the first few plates, an angular resolution with a HEW better than  $5''$ . The plates can also be measured during assembly using a phase-shifting Twyman-Green Interferometer with a Computer Generated Hologram (CGH)<sup>14</sup> (Fig. 3-1).

Now that it has been shown that the plates follow the shape of the mandrel and bond to each other, the main obstacle to achieve stacks, so called High Performance Pore Optics (HPOs), of up to 100 plates, remains particulate contaminants that enter the system in either transport, handling or machining. A trapped particle as small as  $1\mu\text{m}$  creates a void of several mm diameter.

Ribbed plates are transported in a custom built container, chemically cleaned and the stacking process is carried out by a stacking robot in a particle free environment to prevent contamination. Additional methods to remove stray particles are being tested.

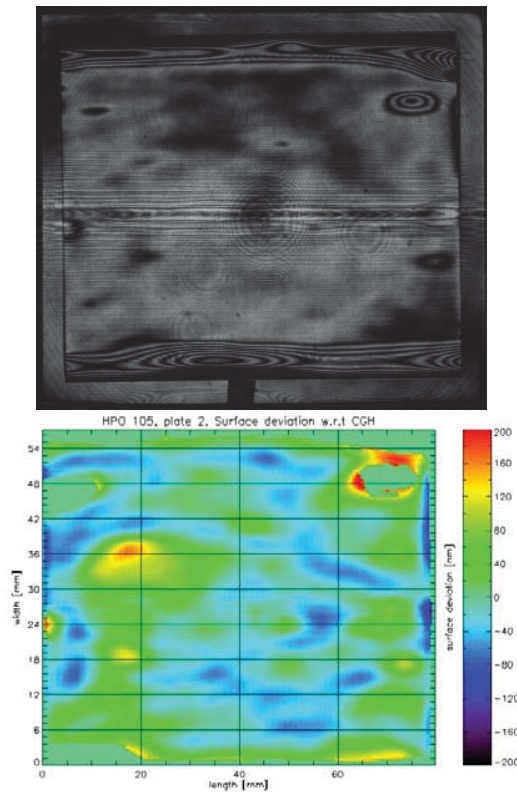


**Fig. 3-1:** Above, interferogram w.r.t. to a CGH, recorded at wavelength 633 nm, on the 2<sup>nd</sup> silicon plate that is stacked onto a Zeiss polished mandrel, which is larger than the plate and also visible. Central horizontal lines are artefacts caused by the CGH. Bottom image shows surface deviation of the same plate w.r.t. the mandrel. 80% of the area is fully bonded and within one fringe. Cylindrical axis is horizontal.

The stacks of silicon plates are built such that they approximate part of half of a Wolter I optic section. By changing the height of the ribs along the optical axis (z-direction) it will be possible to form a conical approximation. Each tandem forms part of the overall x-ray aperture and must be aligned on an optical bench that will form the structure of the optic.

An ongoing activity at ESA is developing both the technology to assemble the mirror stacks, align them in brackets, and develop a structure that can be used to form an aperture. In this case the large aperture, such as could be used for the XEUS telescope, will be formed from a number of “petals”, each petal containing many stacks of aligned tandems, see Fig. 3-2. In the technology development activity 3 tandems are being built and aligned in a CeSiC petal, with mass

dummies occupying the other spaces<sup>12</sup>. CeSiC has been selected as the material for the petal structure following trade-offs considering expected thermal variation across the aperture.

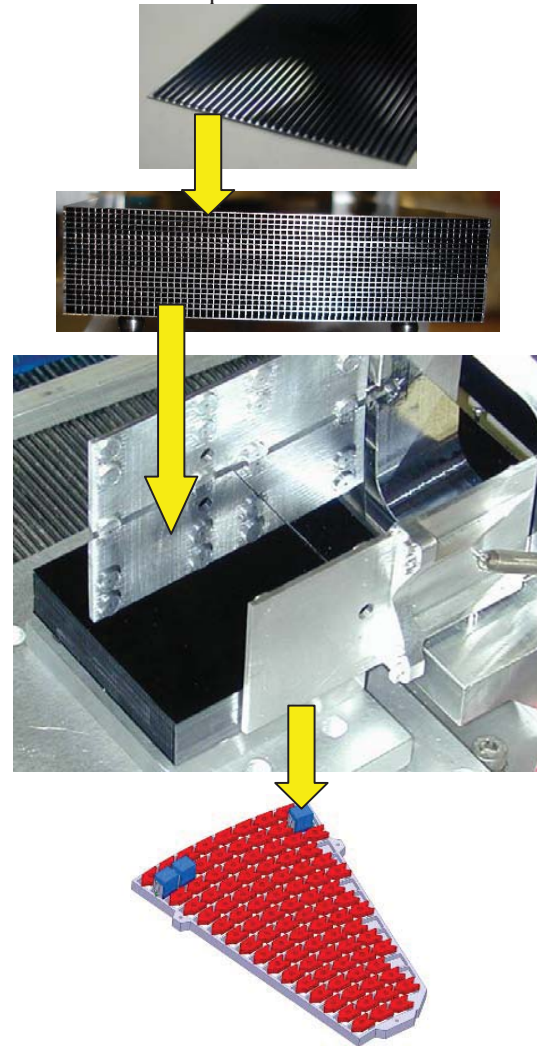


**Fig. 3-2:** Integration concept of silicon pore optics. Ribbed silicon plates (top) are bent and assembled on a mandrel to form porous structures. Two plate stacks are co-aligned and integrated using brackets to form a Wolter-I x-ray lens. Tens of tandems are then integrated into a petal structure (bottom).

Analysis has shown that to reach the goal of a 2” HEW the angle  $\beta$  (Fig. 3-3) has to be set accurately to within 1”, assuming no other errors in alignment, which is very challenging. However, tolerance analysis shows that misalignments in the integration of the two parts of the tandem can largely be compensated for by rotations and translations during integration of the tandem into the petal<sup>10,12</sup>. Only three errors cannot be corrected (translation of the hyperbolic stack in x or y direction or rotation in  $\beta_y$ ) and these would cause a loss in transmission. The remaining 9 axes can be corrected given that equivalent alignment volume for the tandem

can be accommodated in the petal to tandem interface. In effect this increases the volume required by each tandem, thereby reducing the effective area of the overall x-ray aperture. This requires trade-off in the final design of an x-ray telescope.

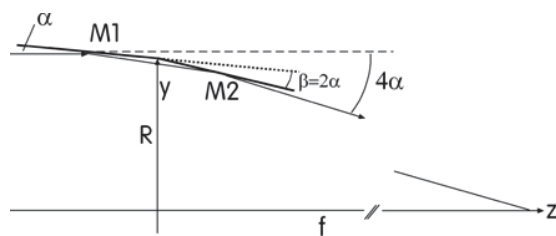


**Fig. 3-3:** Schematic of the Wolter-I configuration. M1 is parabolic, M2 hyperbolic.  $R$  = radius and  $f$  = focal length. X-rays enter from the left side. Petal is in the  $x/y$  plane.

Integration of the first tandem pair of stacks into their bracket mount was recently completed<sup>10</sup>. A 2.8 keV pencil beam, with an initial HEW 3.1", was reflected under a grazing incidence angle of 0.57°, inside pore 31 of the 1<sup>st</sup> plate, and the reflection recorded at a distance of 5 m and a height of 0.2 m, corresponding to the correct setting of the  $4\alpha$  angle at 2.29°, see Fig. 3-4.

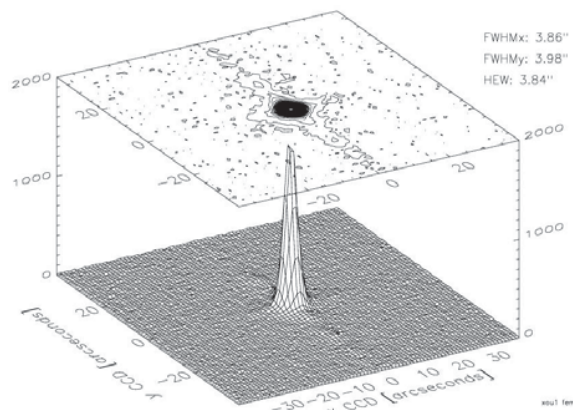


**Fig. 3-4:** First recorded reflection of an x-ray beam imaged by a silicon pore optic, integrated and fixed in Wolter-I configuration<sup>10</sup>.

#### 4. CONCLUSIONS

Two types of x-ray optic have been discussed. It has been shown that glass micro-pore material and silicon milli-pore structures have been demonstrated to form viable x-ray optic components. Both technologies are based on commercially available products and processes. Tests on demonstration lenses have shown that their performance can be acceptable for a lightweight, compact imager in the case of glass and higher resolution and performance in the case of silicon. Tests will continue with both technologies to

align both tandem pairs, to form Wolter I configurations, and integrated, x-ray focusing lenses.

#### 5. ACKNOWLEDGMENTS

The authors wish to express their appreciation to the team of PTB at the BESSY synchrotron in Berlin, for their assistance in x-ray measurement campaigns.

#### 6. REFERENCES

1. "Bepi-Colombo Science Requirements for the Payload of the Mercury Planetary Orbiter", SCI-PB-RS-1156, Version 2.2, ESA, Feb. 2004
2. C. Erd et al, "BepiColombo Payload Study Document", SCI-A/2002/007/Dc/CE, CR\_BC\_TN15, iss. 4, rev. 1, ESA, February 2004
3. M. Bavdaz et al, "Progress at ESA on High Energy Optics technologies", Proc. SPIE, Vol. 5168, pp.136-147 Jan. 2004
4. S. Kraft et al, "Development of x-ray pore optics: novel high-resolution silicon millipore optics for XEUS and ultralow mass glass micropore optics for imaging and timing", Proc. SPIE Vol. 5539, pp. 104-115, Nov. 2004
5. "Development of microchannel plates for UV and x-ray imaging systems", Photonis Summary Report, ESTEC 12193/96/NL/SB, June 2000
6. M. Collon et al, "Metrology for square glass fibres for micropore x-ray optics", EOS Conf. Industrial Imaging and Machine Vision, Munich, June 2005
7. K. Wallace et al, "Development of micro-pore optics for x-ray applications", Proc. of SPIE 5900-36, San Diego, 2005
8. M. Beijersbergen et al, 'Silicon Pore Optics: novel lightweight high-resolution X-ray optics developed for XEUS', Proc. of SPIE 5488-137, San Diego, 2004
9. S. Kraft et al, 'Development of modular High-performance Pore Optics for the XEUS x-ray telescope', Proc. of SPIE-5900-53, San Diego, 2005
10. M. Collon et al, 'Metrology, integration and performance verification of silicon pore optics in Wolter-I configuration', Proc. of SPIE-6266-131, Orlando, 2006
11. K. Wallace et al, "Developments in glass micro pore optics for x-ray applications", Proc. of SPIE-6266-47, Orlando, 2006
12. R. Graue et al, "Design of an X-Ray Telescope Optics for XEUS", ICSO, Noordwijk, 2006
13. R. Günther et al, "Production of Silicon Pore Optics", Proc. of SPIE-6266-46, Orlando, 2006
14. M. Collon et al, "Performance Characterisation of Silicon Pore Optics", Proc. Of SPIE-6266-66, Orlando, 2006